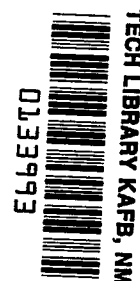


NASA TECHNICAL NOTE



NASA TN D-8252 c.1

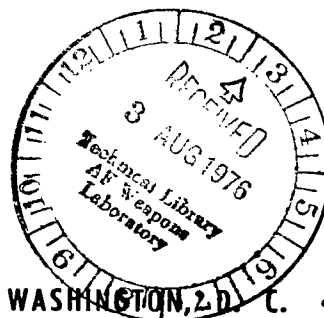
NASA TN D-8252



LOAN COPY: RETI
AFWL TECHNICAL
KIRTLAND AFB, N. M.

FRICITION CHARACTERISTICS OF 20×4.4 ,
TYPE VII, AIRCRAFT TIRES CONSTRUCTED
WITH DIFFERENT TREAD RUBBER COMPOUNDS

Robert C. Dreher and Thomas J. Yager
Langley Research Center
Hampton, Va. 23665



NATIONAL AERONAUTICS AND SPACE ADMINISTRATION • WASHINGTON, D. C. • JULY 1976



0133993

1. Report No. NASA TN D-8252		2. Government Accession No.		3. Recipient's Catalog No.	
4. Title and Subtitle FRICTION CHARACTERISTICS OF 20 x 4.4, TYPE VII, AIRCRAFT TIRES CONSTRUCTED WITH DIFFERENT TREAD RUBBER COMPOUNDS				5. Report Date July 1976	
				6. Performing Organization Code	
7. Author(s) Robert C. Dreher and Thomas J. Yager				8. Performing Organization Report No. L-10825	
				10. Work Unit No. 505-11-41-05	
9. Performing Organization Name and Address NASA Langley Research Center Hampton, Va. 23665				11. Contract or Grant No.	
				13. Type of Report and Period Covered Technical Note	
12. Sponsoring Agency Name and Address National Aeronautics and Space Administration Washington, D.C. 20546				14. Sponsoring Agency Code	
15. Supplementary Notes					
16. Abstract <p>A test program was conducted at the Langley aircraft landing loads and traction facility to evaluate the friction characteristics of 20 x 4.4, type VII, aircraft tires constructed with experimental cut-resistant, tread rubber compounds. These compounds consisted of different blends of natural rubber (NR) and an alfin catalyzed styrene-butadiene copolymer rubber (SBR). One tire having a blend of 30 SBR and 70 NR and another having a blend of 60 SBR and 40 NR in the tread were tested together with a standard production tire with no SBR content in the tread rubber.</p> <p>The results of this investigation indicated that the test tires constructed with the special cut-resistant tread rubber compositions did not suffer any significant degradation in tire friction capability when compared with the standard tire. In general, tire friction capability decreased with increasing speed and surface wetness condition. As yaw angle increased, tire braking capability decreased while tire cornering capability increased. Tread-wear data based on number of brake cycles, however, suggested that the tires with alfin SBR blends experienced significantly greater wear than the standard production tire.</p>					
17. Key Words (Suggested by Author(s)) Tires Friction Tread compound Aircraft			18. Distribution Statement Unclassified - Unlimited Subject Category 05		
19. Security Classif. (of this report) Unclassified	20. Security Classif. (of this page) Unclassified	21. No. of Pages 26	22. Price* \$ 3.75		

FRICION CHARACTERISTICS OF 20×4.4 , TYPE VII, AIRCRAFT TIRES CONSTRUCTED WITH DIFFERENT TREAD RUBBER COMPOUNDS

Robert C. Dreher and Thomas J. Yager
Langley Research Center

SUMMARY

A test program was conducted at the Langley aircraft landing loads and traction facility to evaluate the friction characteristics of 20×4.4 , type VII, aircraft tires constructed with experimental cut-resistant, tread rubber compounds. These compounds consisted of different blends of an alfin catalyzed styrene-butadiene copolymer rubber (SBR) and natural rubber (NR). One tire having a blend of 30 SBR and 70 NR and another having a blend of 60 SBR and 40 NR in the tread were tested together with a standard production tire with no SBR content in the tread rubber.

The results of this investigation indicated that the test tires constructed with the special cut-resistant tread rubber compositions did not suffer any significant degradation in tire friction capability when compared with the standard tire. With respect to braking friction, the tire with the blend of 30 SBR and 70 NR developed the highest values of the three tires tested; the tire with the blend of 60 SBR and 40 NR developed the highest values of cornering friction. In general, tire friction capability decreased with increasing speed and surface wetness condition. As yaw angle increased, tire braking capability decreased while tire cornering capability increased. Tread-wear data based on number of brake cycles, however, suggested that the tires with alfin SBR blends experienced significantly greater wear than the standard production tire. During this test program, tread-wear resistance was also observed to deteriorate with increasing SBR content.

INTRODUCTION

Aircraft tire tread life is an important factor in both the economy and efficiency of commercial and military aircraft operations. As pointed out in reference 1, tire replacement accounts for approximately half the overall landing-gear maintenance costs of current jet airplanes. Generally, the level of tread wear or the extent of tread cuts determines when a tire is to be replaced; however, occasions do arise when tire blowouts and thrown treads necessitate early tire replacement. For many years, aircraft tire manufacturers have been trying to develop tread rubber compounds which resist cutting and improve wear life without compromising design strength or friction capability. (See refs. 2 and 3.)

However, most new tread rubber compounds have proven to be unsatisfactory, primarily because of the tire heat buildup during aircraft landing operations. This tire heat buildup can lead to serious problems associated with ply- or tread-separation, tread throwing or "chunk-out," and even blowout by internal thermal decomposition. Natural rubber has exhibited the most resistance to heating of any practical elastomer examined. Polybutadiene rubber, however, has demonstrated a better abrasion resistance than natural rubber. Achieving an optimum blend of these two elastomers has been the objective of most recent efforts by manufacturers to improve aircraft tire tread life. (See ref. 3.) One such blend, identified as an alfin catalyzed styrene-butadiene copolymer rubber (SBR) mixed with natural rubber (NR), was used in tires constructed by a major tire manufacturer under contract to the United States Air Force (USAF). Dynamometer qualification tests were successfully completed at the Air Force Materials Laboratory, Wright-Patterson Air Force Base, Ohio.

Some low-speed truck tests were conducted on a variety of runway debris (ref. 4) and demonstrated that the alfin SBR tread rubber material had cut-resistant qualities superior to those of the conventional tire tread rubber material. However, an evaluation of the braking and cornering capability of this new tire tread material was required before the material could be used on operating aircraft.

This paper presents the results of a test program conducted at the Langley aircraft landing loads and traction facility to evaluate the friction capability of alfin SBR/NR blended aircraft tires in support of a USAF program to improve aircraft tire tread materials. Two 20×4.4 , 12-ply-rating, type VII tires, each having different blends of the alfin SBR/NR composition in the tread, were tested together with a standard production tire (zero SBR) to define their braking and cornering characteristics. All these tires had a three-groove tread pattern. These braking and cornering characteristics included the drag- and cornering-force friction coefficients which were obtained with the tires operating on dry, damp, and flooded surfaces at yaw angles of 0° , 5.4° , 10.9° , and 16.3° and at ground speeds from 5 to 106 knots (1 knot = 0.5144 m/s). In addition to evaluating the friction capabilities of the tires, the test program monitored tire tread wear.

The tires, wheels, and brake assembly used in the tests were supplied by the U.S. Air Force (Alfin SBR Tire Test, AF-AM-409).

SYMBOLS

Values are given in both SI and U.S. Customary Units. The measurements and calculations were made in U.S. Customary Units. Factors relating the two systems are presented in reference 5.

p	tire inflation pressure, kPa (psi)
V	ground speed, knots
μ_d	drag-force friction coefficient parallel to direction of motion, $\frac{\text{Drag force}}{\text{Vertical force}}$
$\mu_{d,\max}$	maximum drag-force friction coefficient
$\mu_{d,\text{skid}}$	skidding drag-force friction coefficient
μ_s	cornering-force friction coefficient perpendicular to direction of motion, $\frac{\text{Side force}}{\text{Vertical force}}$
$\mu_{s,\max}$	maximum cornering-force friction coefficient

TEST APPARATUS AND PROCEDURE

Tires

The test tires for this investigation were three-groove, 20×4.4 , 12-ply-rating, type VII, aircraft tires similar to those used on a jet trainer aircraft. The tread rubber material was based on blends of alfin catalyzed styrene-butadiene copolymer rubber (SBR) and natural rubber (NR). Tread rubber compositions based on ratios of alfin SBR to NR of 30/70 and 60/40 (hereafter referred to as 30/70 SBR/NR and 60/40 SBR/NR) were fabricated on two sets of the 20×4.4 aircraft tires. In addition to these tires, a standard production tire with an identical tread groove pattern but without any SBR content in its tread rubber was also evaluated. All tire carcasses were of identical construction. A photograph of one of the test tires is shown in figure 1 together with a static tire footprint obtained at the test vertical load and tire inflation pressure. No significant difference was observed in the footprints obtained from each of the three test tires. The friction performances of the three test tires were evaluated at a vertical load of 22.4 kN (5000 lbf) with an inflation pressure p of 1551 kPa (225 psi).

Test Surfaces

For this investigation, approximately equal segments of a 183-m (600-ft) section of the concrete test runway were maintained in dry, damp, and flooded conditions. For the damp condition, the surface was wetted to a depth of less than 0.03 cm (0.01 in.); the water depth for the flooded surface ranged from 0.5 to 0.8 cm (0.2 to 0.3 in.). Photographs of the three segments ready for test are presented in figure 2. Surface texture-depth values (an

indication of potential frictional characteristics) were measured by the grease sample technique described in reference 6. The measured values indicated that the dry concrete test surface had an average depth of $91\text{ }\mu\text{m}$ (0.0036 in.), the damp concrete section had an average depth of $114\text{ }\mu\text{m}$ (0.0045 in.), and the flooded test section had an average depth of $145\text{ }\mu\text{m}$ (0.0057 in.).

Some rubber was deposited on the pavement in the dry test area, however, as a result of the tire brake cycles. (See dry surface photograph in fig. 2.) These deposits effectively reduced the surface texture depth, and when the entire surface was coated, removal of this rubber buildup and cleaning of the surface were necessary before continuing the test runs. A chemical agent together with a high pressure water jet expelled from a hand-held hose nozzle removed all the bulk rubber and restored the surface texture depth to its original clean surface value. Because of the surface wetness, tire rubber deposits did not adhere to the damp and the flooded surfaces during brake cycles.

Test Facility

The test program was conducted at the Langley aircraft landing loads and traction facility described in references 7 and 8. The test tire and the wheel and brake assembly were mounted on a dynamometer attached to the front of the small test carriage as shown in figure 3. A closeup view is presented in figure 4. The instrumented dynamometer (shown schematically in fig. 5) consisted of load beams to measure drag, vertical, and lateral forces and links to measure brake torque. All measurements were made at the wheel axle. Instrumentation was also provided to measure brake pressure, test wheel velocity, and carriage horizontal displacement and forward speed. Continuous time histories of the output of the instrumentation during a run were obtained by tape recorders mounted on the test carriage.

Test Procedure

The procedure followed for most test runs involved (1) propelling the carriage to the desired ground speed; (2) releasing the drop test fixture to apply the preselected vertical load on the tire; and (3) subjecting the tire to brake cycles on first the dry surface and, subsequently, on the damp and flooded surfaces. A cycle began when the brake pressure valve was actuated, thereby braking the tire from a free-rolling condition to a locked-wheel skid. An entire cycle took place within each runway test segment. Immediately after wheel lockup, the brake was released to allow tire spin-up prior to the next cycle on the next segment. Brake-cycle location on the damp and flooded surfaces was not varied during the test program. However, because of the tire rubber deposits from skids on the dry surface, the point of brake application on that surface was varied between runs in an attempt to brake the tire in a clean area each time. For each test

tire series, braking runs were conducted at preset yaw angles of 0° , 5.4° , 10.9° , and 16.3° ; the yaw angles were held constant for each test run. Carriage speeds for these tests ranged from 5 to 106 knots. The 5-knot speed was obtained by towing the carriage with a ground vehicle; for the higher speeds, the carriage was propelled by the hydraulic jet as described in reference 7.

RESULTS AND DISCUSSION

General

Figure 6 presents typical time histories of the significant parameters obtained during a single brake cycle. These parameters include the test wheel slip ratio (ratio of axle horizontal velocity minus tire peripheral velocity to axle horizontal velocity); the tire-to-ground forces (corrected for inertia) in the drag, vertical, and side directions; and the brake pressure and resulting torque. Time histories of the drag-force friction coefficient parallel to the direction of motion μ_d and the cornering-force friction coefficient perpendicular to the direction of motion μ_s are also presented. Both coefficients are computed from the measured force data. In the example shown in figure 6, brakes were applied at time 0.4 sec and a complete wheel lockup resulted approximately 0.2 sec later. During the wheel spin-down period of less than 0.1 sec, μ_d peaked and then diminished with decreasing wheel speed while μ_s rapidly decreased to zero as the wheel approached lockup. This wide variation in tire braking and cornering friction with brake application is more clearly indicated in figure 7. The drag- and side-force friction coefficients measured during the dry brake cycle (fig. 6) are replotted in figure 7 as a function of wheel slip ratio. These computer plots also illustrate how the data were faired for evaluating the variation of both drag-force and cornering-force friction coefficients with wheel slip ratio.

For each test condition, the time-history data obtained during a brake cycle were faired (see fig. 6) to determine: (a) the maximum drag-force friction coefficient $\mu_{d,max}$ encountered during wheel spin-down; (b) the skidding drag-force friction coefficient $\mu_{d,skid}$ measured during wheel lockup; and (c) the maximum cornering-force friction coefficient $\mu_{s,max}$ before braking was initiated. The values thus generated for the three test tires were compiled for each test surface and are presented in table I.

In the following sections, the friction characteristics of the three test tires are evaluated on the basis of μ_d and μ_s variations with slip ratio on dry, damp, and flooded surfaces. (See fig. 8.) The variations of $\mu_{d,max}$, $\mu_{d,skid}$, and $\mu_{s,max}$ with ground speed and with yaw angle are shown in figures 9 and 10, respectively. It should be pointed out that the values for $\mu_{d,skid}$ and $\mu_{s,max}$ in figures 9 and 10 were determined from

fairings of a relatively long time duration before braking to obtain $\mu_{s,max}$, and after the wheel had locked up, to obtain $\mu_{d,skid}$. (See fig. 6.) Since the corresponding values of μ_s and μ_d in figure 8 were essentially instantaneous values and were computer selected at a constant data sample rate, some differences in the magnitude of these coefficients do exist between the two sets of data.

Variation of Friction Characteristics With Slip Ratio

The typical variation of the drag-force friction coefficient μ_d and cornering-force friction coefficient μ_s with slip ratio for the three test tires on dry, damp, and flooded surfaces is presented in figure 8. The variation extends from a free-rolling condition (slip ratio = 0) to a locked-wheel condition (slip ratio = 1.0) and was obtained at a nominal ground speed V of 100 knots and a yaw angle of 10.9° . The curves of these figures are based on fairings of computer plots similar to that shown in figure 7. The curves represent fractions of a second in real time as illustrated by the brake-cycle time histories of figure 6 where approximately one-tenth of a second was required for the wheel to spin down completely. The data which illustrate the dry tire friction (fig. 8(a)) exhibit the classical variation in drag-force friction coefficient with slip ratio: μ_d increases with brake application from the free-rolling value, reaches a maximum, and then decreases to lower levels as the wheel approaches and reaches lockup. (See refs. 9 and 10.) The figure shows that μ_d peaks before a slip ratio of 0.2 for all three tires at a yaw angle of 10.9° whereas the cornering-force friction coefficient μ_s varies from a maximum value during free roll to zero at or appreciably before the wheel locks up. A comparison of the braking and cornering friction curves obtained with each test tire on the dry surface reveals that the standard production tire developed the highest μ_d and that the 60/40 SBR/NR tire was the only test tire to maintain some cornering until the wheel locked.

The variation of both μ_d and μ_s on the damp and flooded surfaces (figs. 8(b) and 8(c), respectively) is similar to that observed on the dry surface. However, as might be expected, the magnitude of these friction coefficients is considerably reduced and the peak μ_d not nearly as well defined. On both of these wet surfaces, the 30/70 SBR/NR tire consistently developed significantly higher values of μ_d . The corresponding μ_s curves indicate that the cornering capability of all three tires is greatly reduced or completely lost at or before wheel lockup. It is of interest to note that in the μ_s curves of figure 8, the 60/40 SBR/NR tire was the only test tire at a yaw angle of 10.9° to maintain some cornering capability until the wheel locked up on all test surface conditions. Tire friction data (see table I) obtained at other test yaw angles exhibited trends similar to those illustrated in the curves of figure 8.

Variation of Friction Characteristics With Ground Speed

The effect of ground speed on certain tire braking and cornering characteristics which were developed during operations on dry, damp, and flooded surfaces is shown in figure 9 for each test tire at yaw angles of 0° and 16.3° . It should be noted that similar trends were observed in the tire friction data obtained at yaw angles of 5.4° and 10.9° . (See table I.) As a matter of interest, data obtained on areas of the dry surface test section which contained rubber deposits from previous braking cycles are also included in figure 9. The rubber contamination greatly reduced the tire friction during braking.

Maximum drag-force friction coefficient.- The data of figure 9 indicate that the maximum drag-force friction coefficient $\mu_{d,max}$ decreases with increasing ground speed for all three tires. The decrease was observed under all runway surface conditions although it is much less pronounced on the dry than on the two wetted surfaces; this trend corroborates those observed in references 11 to 14. The magnitude of $\mu_{d,max}$ developed by the 30/70 SBR/NR tire is generally the highest of the three tires tested.

Values of $\mu_{d,max}$ were, in general, higher on the flooded test surface than on the damp surface for similar speeds and yaw angles. Two factors may contribute to the high $\mu_{d,max}$ level on the flooded surface. First, the texture depth of the flooded surface is approximately 25 percent greater than that of the damp surface. This greater texture depth should affect the tire friction at speeds at least up to 100 knots since that speed is well below the computed dynamic hydroplaning speed of 135 knots for the test tire (ref. 11). Second, the flooded surface, because of its water depth, induces a significant fluid drag on the tire, but such drag is negligible on the damp surface with no standing water.

Skidding drag-force friction coefficient.- The skidding drag-force friction coefficient $\mu_{d,skid}$ shown in figure 9 decreases with increasing ground speed for all three tires in a manner similar to that of $\mu_{d,max}$ but at somewhat lower friction levels. This trend is noted at all test yaw angles and on the dry, damp, and flooded surfaces. Values of $\mu_{d,skid}$ on the flooded surface are shown to be equal to or slightly higher than those on the damp surface, particularly at the higher ground speeds. This variation apparently results from the same reasons identified in the preceding section. Little difference appears to exist in the magnitude of $\mu_{d,skid}$ developed by each of the test tires at similar speeds and yaw angles on all runway surface conditions (see table I); however, the 30/70 SBR/NR tire again appears to provide slightly higher values.

Maximum cornering-force friction coefficient.- The data in figure 9(a) indicate, as expected, that the side-force friction coefficient is zero for an unyawed tire under any surface condition. At 16.3° , the data of figure 9(b) indicate that the tire cornering capability on a dry surface is essentially equal to $\mu_{d,max}$ at 5 knots and is also insensitive to speed. Table I shows this trend to be true for the other two test yaw angles. On the damp and flooded surfaces, however, the values of $\mu_{s,max}$ decrease rapidly with increasing ground

speed. The comparative low and high speed cornering friction data obtained with the two alfin SBR tires at 16.3° yaw indicate that the 60/40 SBR/NR tire developed the highest values of $\mu_{s,max}$ on the three test surfaces.

Variation of Friction Characteristics With Yaw Angle

The data of table I are plotted in figure 10 to show the effect of yaw angle on the drag- and cornering-force friction coefficients developed by the test tires at various surface wetness conditions and at nominal ground speeds of 5 and 100 knots.

Maximum drag-force friction coefficient.- The data presented in figure 10 indicate that the highest values of $\mu_{d,max}$ occur for the unyawed tire and generally decrease with increasing yaw angle. Figure 10 more clearly illustrates that a higher level of $\mu_{d,max}$ was obtained with the 30/70 SBR/NR tire than with the other two test tires, particularly on the damp and flooded surfaces. The $\mu_{d,max}$ data for all three tires for flooded conditions are somewhat higher than the respective $\mu_{d,max}$ data for damp conditions because of the fluid drag and surface texture effects discussed in the preceding sections.

Skidding drag-force friction coefficient.- Yaw angle appears to have very little effect on $\mu_{d,skid}$, and at the higher test speeds (fig. 10(b)), the skidding friction coefficient values seem to be insensitive to tread rubber compound. The data in figure 10 show that values of $\mu_{d,skid}$ remain nearly constant throughout the range of yaw angles tested although a reduction in $\mu_{d,skid}$ with increasing ground speed is shown. The values of $\mu_{d,skid}$ on the damp and flooded surfaces are about equal but slightly less than those developed on the dry surface because of thin film lubrication provided by the presence of water.

Maximum cornering-force friction coefficient.- The maximum cornering-force friction coefficient $\mu_{s,max}$ developed by the three tires increases with increasing yaw angle up to and including the maximum test yaw angle on all test surfaces at the low speed of 5 knots. At 100 knots, $\mu_{s,max}$ levels developed by the three test tires appear to reach a peak before a yaw angle of 16.3° on the damp surface. At low speed (see fig. 10(a)), surface wetness conditions do not significantly affect the $\mu_{s,max}$ values, but at high speed (see fig. 10(b)), $\mu_{s,max}$ levels are reduced with increasing surface wetness. In a comparison of the cornering friction developed by the three test tires at yaw angles from 0° to 16.3° (see table I), it was found that the $\mu_{s,max}$ levels of the 60/40 SBR/NR tire tend to be the highest for all test conditions.

Tread-Wear Considerations

During the course of this experimental program, tire tread wear was also monitored by measuring the depth of each tread groove at several positions around the tire circumference after each braking test. When these values were compared with the initial depth

reading, the amount of tread wear could be determined. However, it was difficult to use this information to form the basis for comparing the wear resistance of each tire because the tires were not exposed to identical test conditions (e.g., ambient temperature, speed, length of each brake cycle, yawed rolling distance, and extent of surface contamination). However, a reasonably valid comparison of the tread wear experienced by each tire can be obtained by using a wear index based on the total wear measurement divided by the total number of brake cycles for a given tire. For the standard production tire, this tread-wear per brake-cycle computation resulted in a value of 0.0356 mm/cycle (0.0014 in./cycle). With a tread-wear index of 1.0 assigned to this standard tire-wear per brake-cycle value, similar computations were made for the other two test tires, and comparative tread-wear index numbers were determined. The tread-wear index was 2.15 for the 30/70 SBR/NR tire and 3.94 for the 60/40 SBR/NR tire. These tread-wear index values indicate that the tires with alfin SBR blends experienced significantly greater wear from brake cycles than the standard production tire with no SBR content in the tread rubber. The tread-wear index values also suggest that the wear resistance deteriorates with increasing SBR content.

The phenomena which take place during tire tread cutting and tearing and during tire tread wear (such as that caused by braking under yawed wheel conditions) are not well understood. These alfin SBR tires have proved their good cut and tear resistance (see ref. 4), but it is indeed possible that a tread rubber with good cut and tear resistance does not necessarily possess good wear resistance. An additional program to investigate and define the tread-wear characteristics of these tires would be of interest and may be considered necessary prior to the use of the tires on operating aircraft.

CONCLUDING REMARKS

A test program was conducted at the Langley aircraft landing loads and traction facility to evaluate the friction characteristics of 20×4.4 , type VII, aircraft tires constructed with cut-resistant, tread rubber compounds. Two tires, each with a different blend of alfin catalyzed styrene-butadiene copolymer rubber (SBR) and natural rubber (NR) in its tread composition, were tested together with a standard tire with no SBR content in the tread rubber. The investigation consisted of braking tests from free roll to locked-wheel skids on dry, damp, and flooded runway surfaces at ground speeds from 5 to 106 knots and at yaw angles from 0° to 16.3° .

The results from these tests indicated that the tires constructed with the special, cut-resistant blends of SBR and NR suffer no degradation in friction capability in comparison to a standard tire. Of the tires tested, the highest braking friction values were obtained with the tire having the 30 to 70 ratio of SBR to NR, and the highest cornering friction values were developed by the tire having the 60 to 40 ratio of SBR to NR. In general, the braking capability of all tires was found to decrease with increased ground

speed and surface water depth; further, the maximum available braking coefficient decreased with increased yaw angle whereas the somewhat lower skidding coefficient appeared to be insensitive to yaw angle changes. The tire steering or cornering friction was at a maximum when the wheel was freely rolling but decreased rapidly with braking, reaching zero at or before wheel lockup. Wetting the surface or increasing the ground speed generally tended to decrease the tire cornering capability.

The total tread loss when related to the number of brake cycles for each tire throughout the entire test program suggests that the tires with alfin SBR blends experienced significantly greater wear rates than the conventional rubber-tread tire. In addition, tread-wear resistance appears to deteriorate with increasing SBR content.

Langley Research Center
National Aeronautics and Space Administration
Hampton, Va. 23665
May 10, 1976

REFERENCES

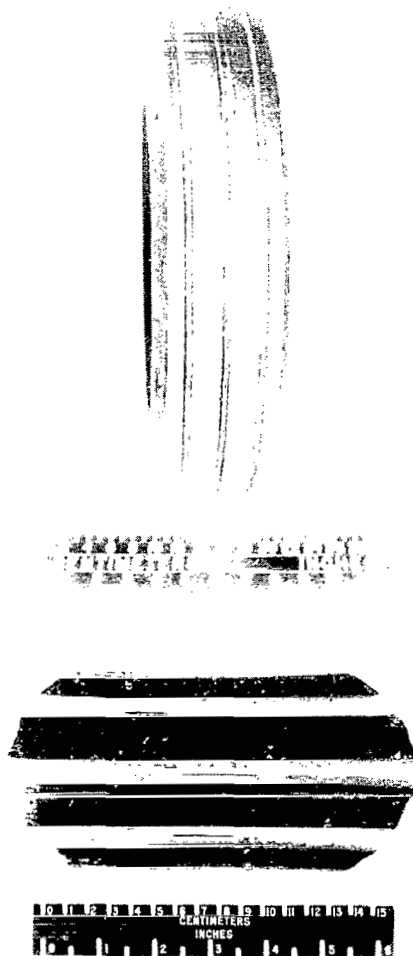
1. McCarty, John Locke: Wear and Related Characteristics of an Aircraft Tire During Braking. NASA TN D-6963, 1972.
2. Clark, Samuel K., ed.: Mechanics of Pneumatic Tires. NBS Monogr. 122, U.S. Dep. Commer., Nov. 1971.
3. Peterson, R. F., Jr.; Eckert, C. F.; and Carr, C. L.: Tread Compound Effects in Tire Traction. The Physics of Tire Traction - Theory and Experiment, Donald F. Hays and Alan L. Browne, eds., Plenum Press, 1974, pp. 223-239.
4. Sapper, D. I.; Hermon, W. C.; and Jennings, G. L.: Aircraft Tire Tread Materials With Extreme Cut, Tear and Abrasion Resistance. AFML-TR-72-261, U.S. Air Force, Oct. 1972. (Available from DDC as AD 908 576L.)
5. Metric Practice Guide. E 380-72, American Soc. Testing & Mater., June 1972.
6. Leland, Trafford J. W.; Yager, Thomas J.; and Joyner, Upshur T.: Effects of Pavement Texture on Wet-Runway Braking Performance. NASA TN D-4323, 1968.
7. Joyner, Upshur T.; and Horne, Walter B.: Considerations on a Large Hydraulic Jet Catapult. NACA TN 3203, 1954. (Supersedes NACA RM L51B27.)
8. Joyner, Upshur T.; Horne, Walter B.; and Leland, Trafford J. W.: Investigations on the Ground Performance of Aircraft Relating to Wet Runway Braking and Slush Drag. AGARD Rep. 429, Jan. 1963.
9. Smiley, Robert F.; and Horne, Walter B.: Mechanical Properties of Pneumatic Tires With Special Reference to Modern Aircraft Tires. NASA TR R-64, 1960. (Supersedes NACA TN 4110.)
10. Horne, Walter B.; and Leland, Trafford J. W.: Influence of Tire Tread Pattern and Runway Surface Condition on Braking Friction and Rolling Resistance of a Modern Aircraft Tire. NASA TN D-1376, 1962.
11. Horne, Walter B.; and Dreher, Robert C.: Phenomena of Pneumatic Tire Hydroplaning. NASA TN D-2056, 1963.
12. Horne, Walter B.; Yager, Thomas J.; and Taylor, Glenn R.: Review of Causes and Alleviation of Low Tire Traction on Wet Runways. NASA TN D-4406, 1968.
13. Dreher, Robert C.; and Tanner, John A.: Experimental Investigation of the Braking and Cornering Characteristics of $30 \times 11.5-14.5$, Type VIII, Aircraft Tires With Different Tread Patterns. NASA TN D-7743, 1974.
14. Leland, Trafford J. W.; and Taylor, Glenn R.: An Investigation of the Influence of Aircraft Tire-Tread Wear on Wet-Runway Braking. NASA TN D-2770, 1965.

TABLE I.- SUMMARY OF FRICTION COEFFICIENTS OBTAINED FOR VARIOUS TEST CONDITIONS

[Tire inflation pressure, 1551 kPa (225 psi); vertical load, 22.4 kN (5000 lbf);
styrene-butadiene rubber (SBR); natural rubber (NR)]

Tire tread SBR/NR ratio	Yaw angle, degrees	Ground speed, knots	Dry surface			Damp surface			Flooded surface		
			$\mu_{d,max}$	$\mu_{d,skid}$	$\mu_{s,max}$	$\mu_{d,max}$	$\mu_{d,skid}$	$\mu_{s,max}$	$\mu_{d,max}$	$\mu_{d,skid}$	$\mu_{s,max}$
Standard (zero SBR)	0	5	0.50	0.43	0	0.40	0.35	0	0.45	0.39	0
	0	22	.48	.30	0	.41	.22	0	.30	.24	0
	0	43	^a .20	^a .10	0	---	.15	0	---	.20	0
	0	67	^a .18	^a .05	0	.30	.09	0	.17	.16	0
	0	76	^a .26	^a .05	0	.22	.07	0	.14	.10	0
	0	103	.40	.15	0	.15	.06	0	.13	.09	0
	5.4	5	.50	.40	.19	.34	.34	.21	.45	.35	.21
	5.4	106	.34	.12	.21	.13	.09	.12	.10	.10	.06
	10.9	5	.44	.41	.39	.38	.39	.34	---	---	.34
	10.9	106	.29	.11	.36	.11	.06	.15	.10	.09	.08
	16.3	5	.41	.41	.45	.35	.35	.40	.39	.39	.39
	16.3	25	.35	.28	.45	.25	.22	.25	.29	.25	.34
	16.3	52	.30	.20	.45	.18	.12	.20	.19	.15	.23
	16.3	72	.30	.16	.45	.14	.14	.20	.15	.13	.19
	16.3	99	.27	.12	.45	.14	.09	.15	.15	.12	.12
	16.3	102	---	---	.45	.13	.10	.17	.10	.10	.10
30/70	0	5	0.55	0.49	0	0.52	0.45	0	0.55	0.50	0
	0	14	.52	.39	0	.42	.32	0	.49	.40	0
	0	40	.52	.26	0	.27	.19	0	.29	.24	0
	0	65	.47	.21	0	.20	.12	0	.35	.16	0
	0	87	.49	.20	0	.22	.10	0	.25	.13	0
	5.4	5	.51	.44	.17	.41	.40	.17	.50	.45	.17
	10.9	5	.45	.45	.34	.43	.36	.33	.49	.47	.34
	10.9	100	^a .31	.16	.30	.15	.11	.14	.15	.11	.05
	16.3	5	.45	.45	.40	.41	.36	.40	.47	.47	.44
	16.3	98	^a .18	.15	.40	.17	.10	.16	.20	.14	.10
60/40	0	5	0.55	0.48	0	0.34	0.34	0	0.46	0.45	0
	0	20	.45	.30	0	.30	.26	0	.40	.30	0
	0	44	.45	.20	0	.21	.15	0	.30	.20	0
	0	63	.38	.17	0	.20	.14	0	.32	.16	0
	0	103	.36	.16	0	.13	.08	0	.15	.11	0
	5.4	5	.50	.43	.25	.33	.33	.23	.40	.37	.24
	5.4	105	.35	.15	.25	.09	.06	.17	.08	.08	.06
	10.9	5	.44	.44	.44	.34	.34	.35	.40	.38	.42
	10.9	105	.22	.14	.45	.09	.06	---	.10	.10	.10
	16.3	5	.44	.44	.50	.36	.36	.43	.43	.40	.48
	16.3	100	.25	.15	.48	---	---	.22	.11	.11	.12

^aValues obtained on surface rubber deposits.



L-76-194

Figure 1.- Profile and footprint of three-groove, 20×4.4 , type VII, test tire. Tire inflation pressure = 1551 kPa (225 psi); Vertical load = 22.4 kN (5000 lbf).

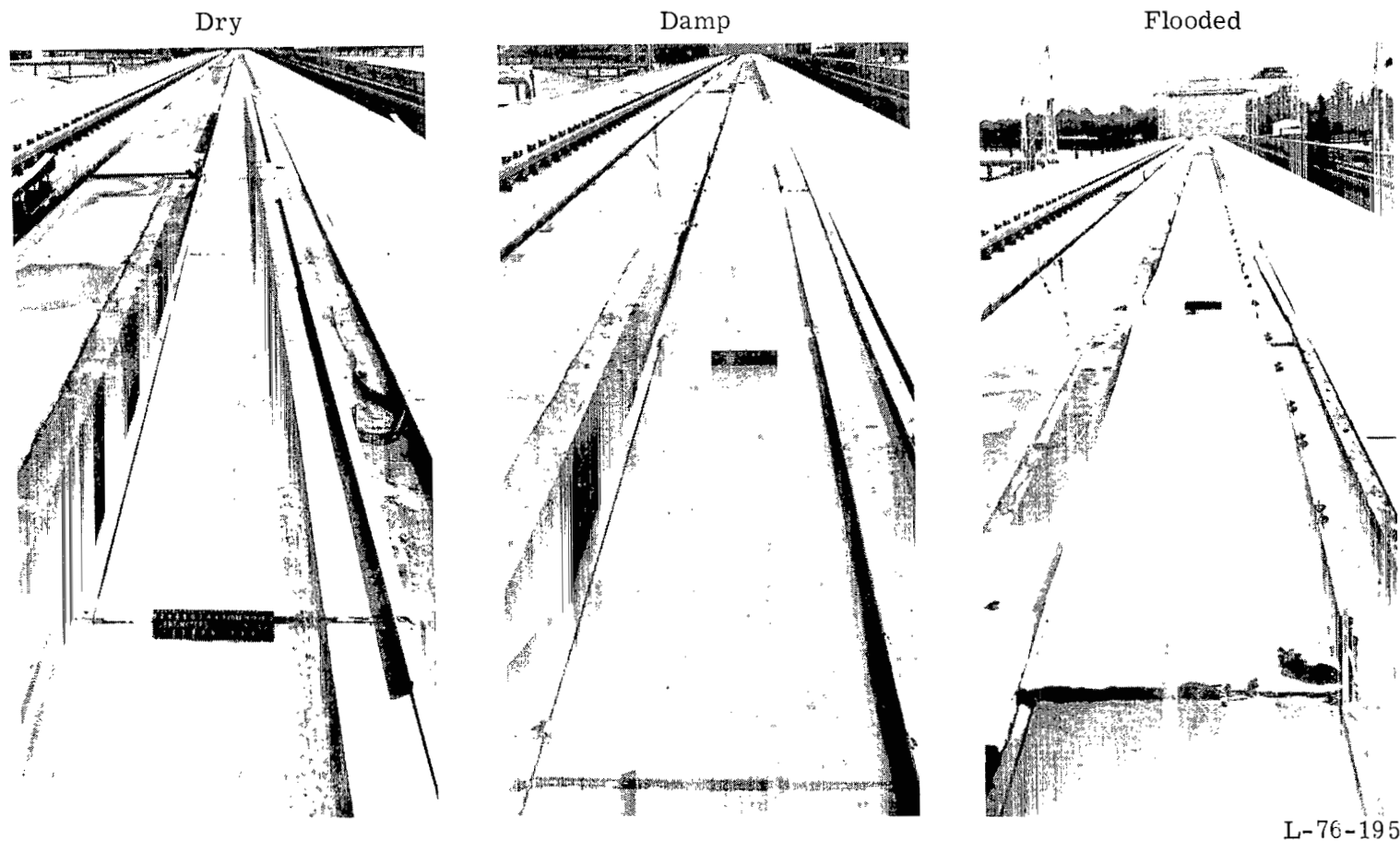
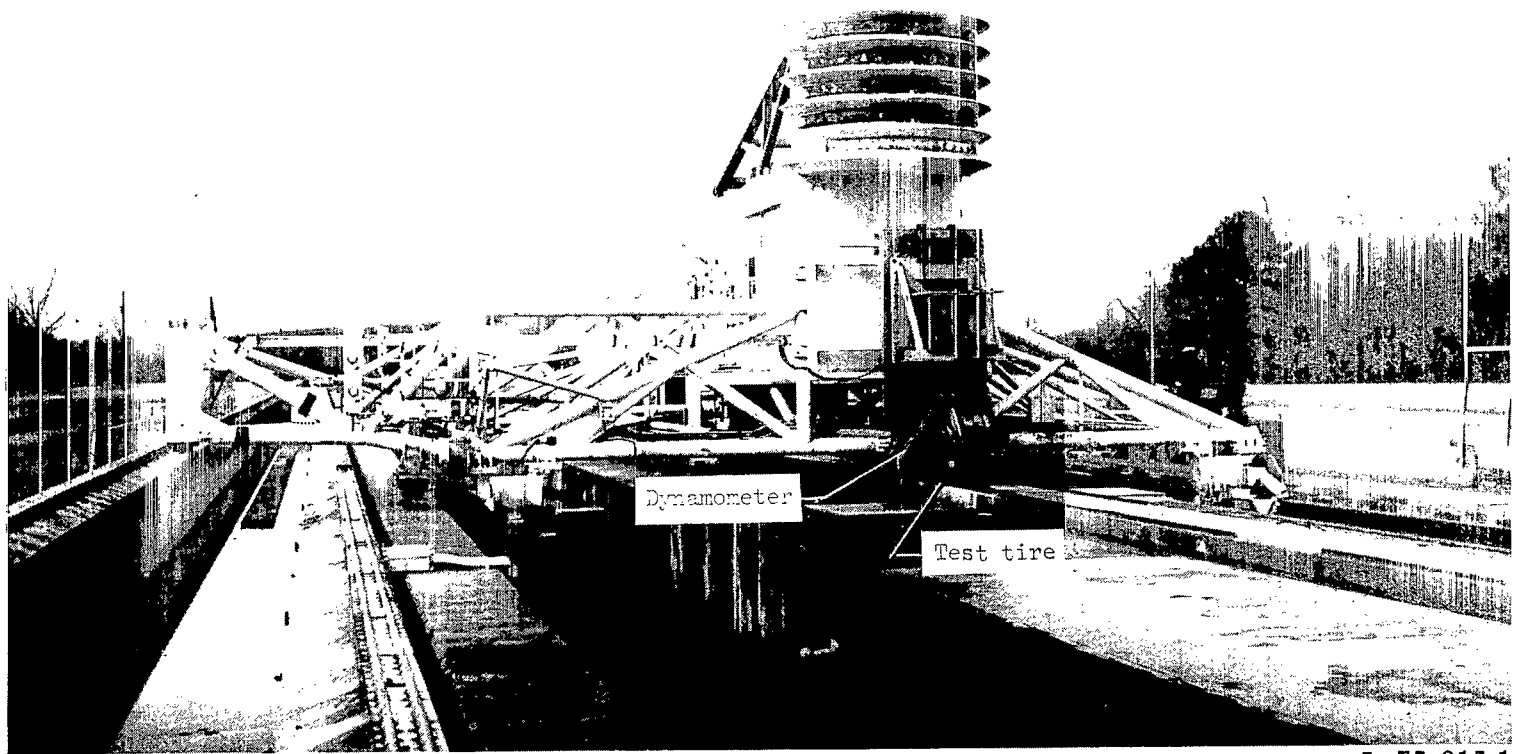
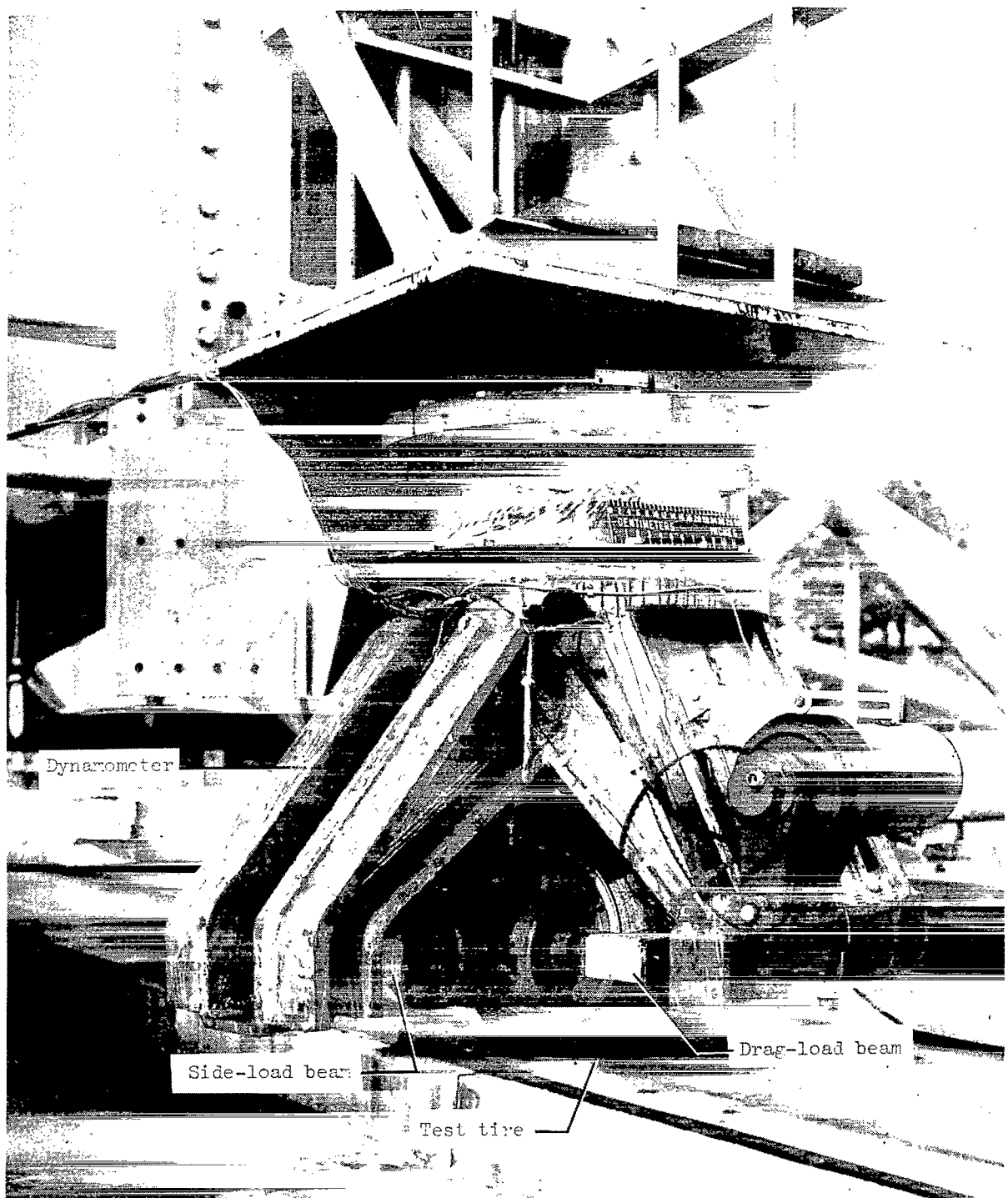


Figure 2.- Runway surface conditions maintained for each test run.



L-75-915.1

Figure 3.- Photograph showing dynamometer mounted on test carriage.



L-75-918.1

Figure 4.- Closeup of test tire installed on dynamometer.

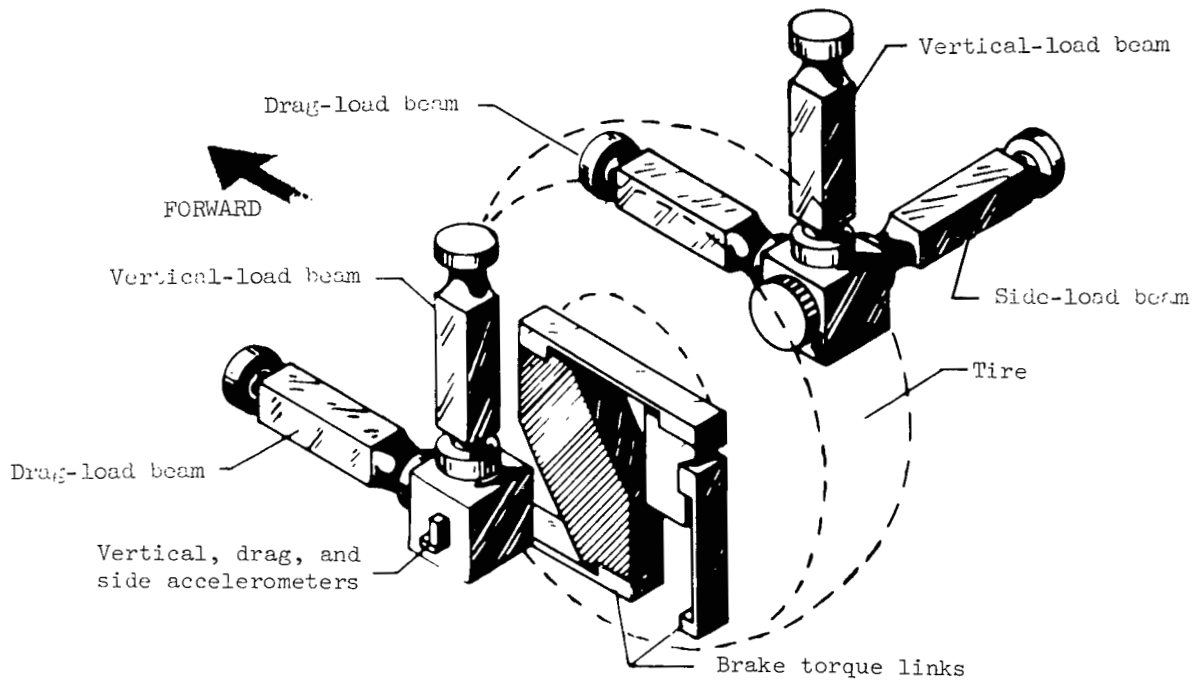


Figure 5.- Schematic of dynamometer used in tests.

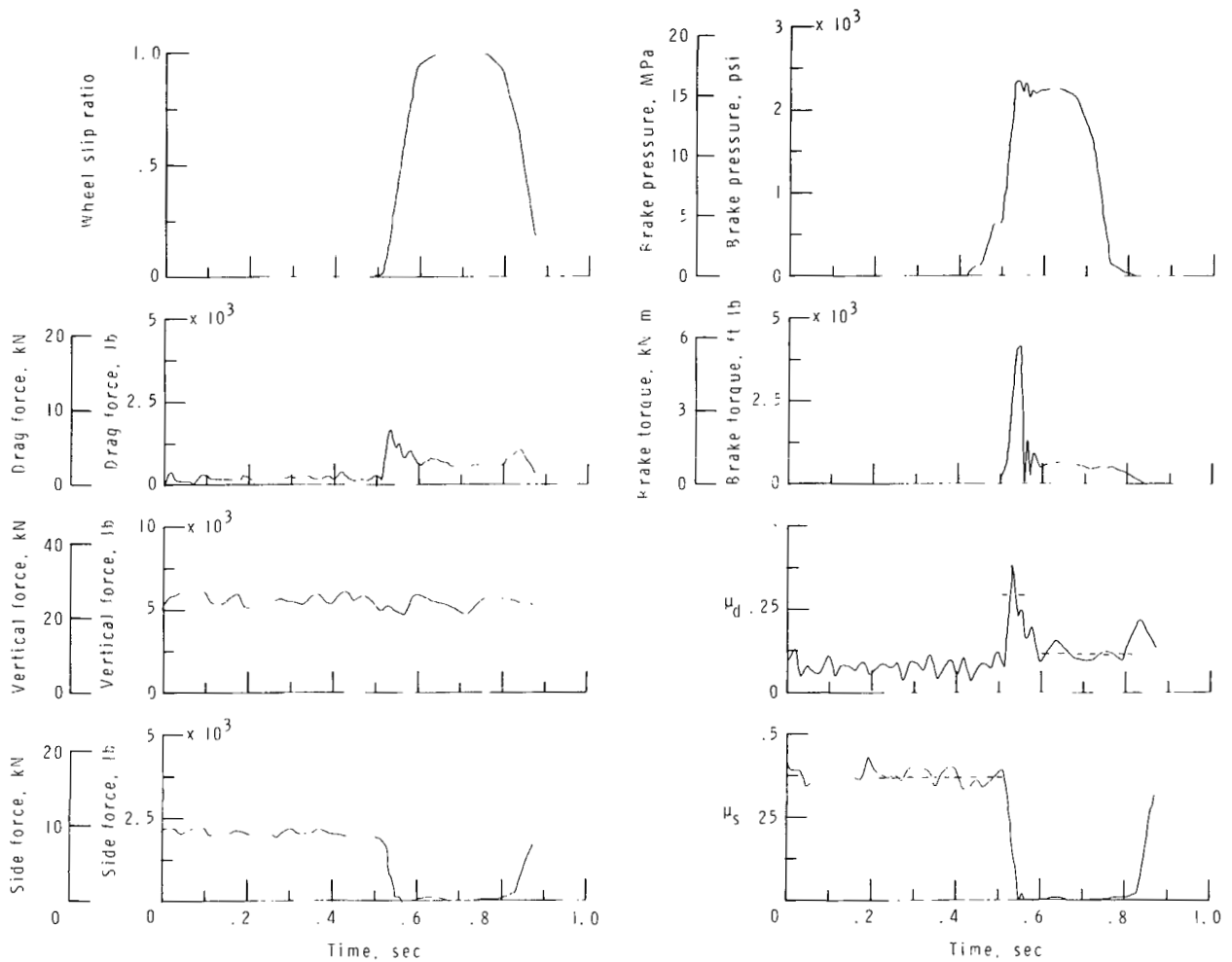


Figure 6.- Typical time histories of various parameters computed for test run brake cycles. Yaw angle, 10.9° ; ground speed, 106 knots; dry concrete surface.

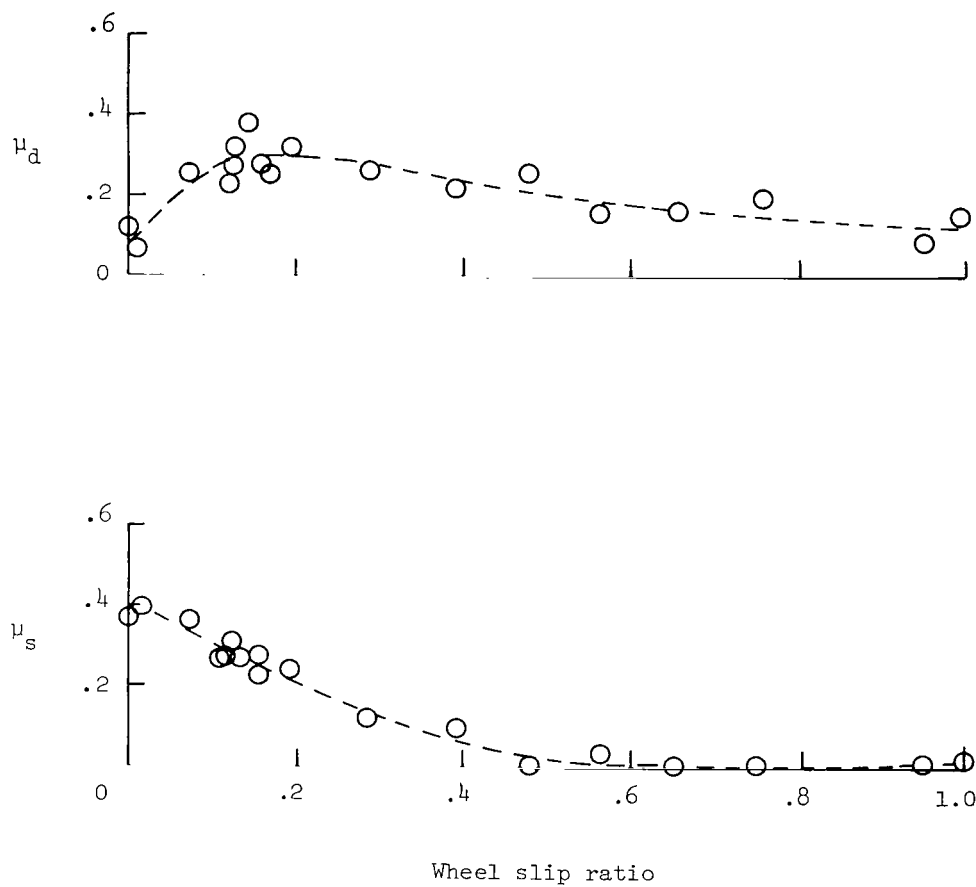
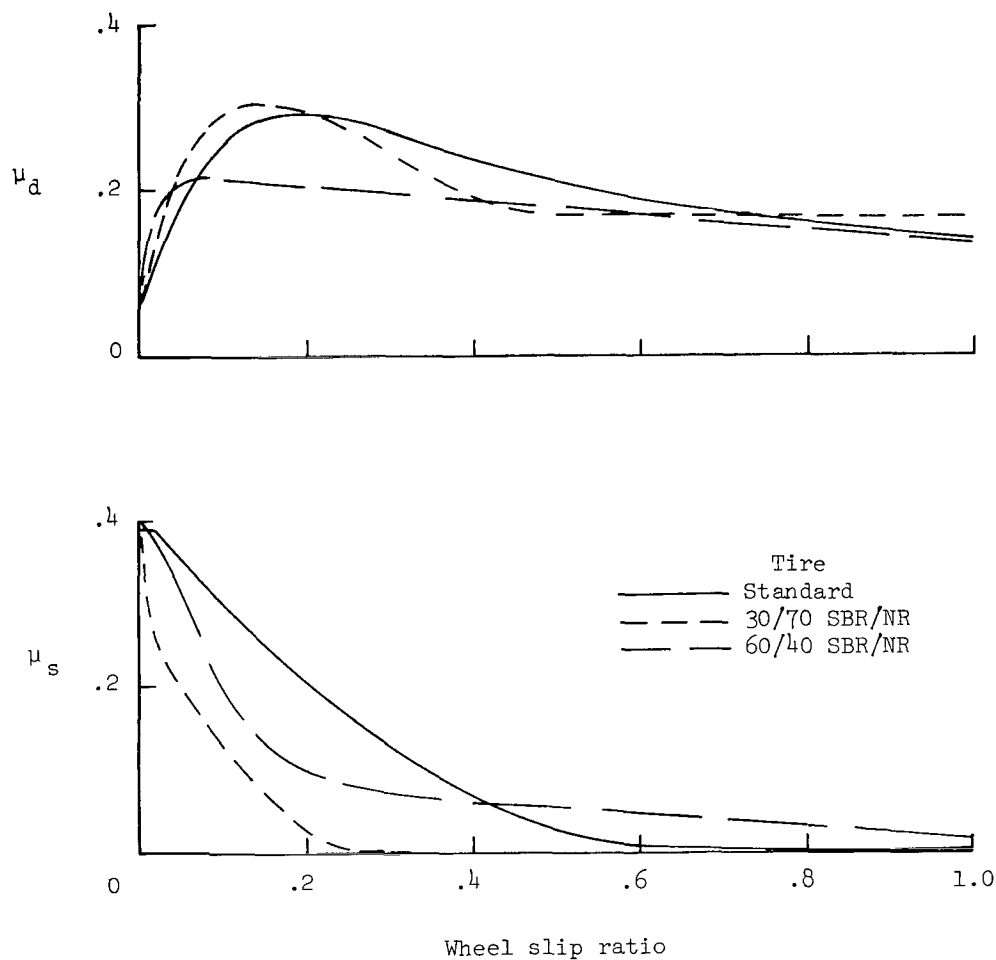
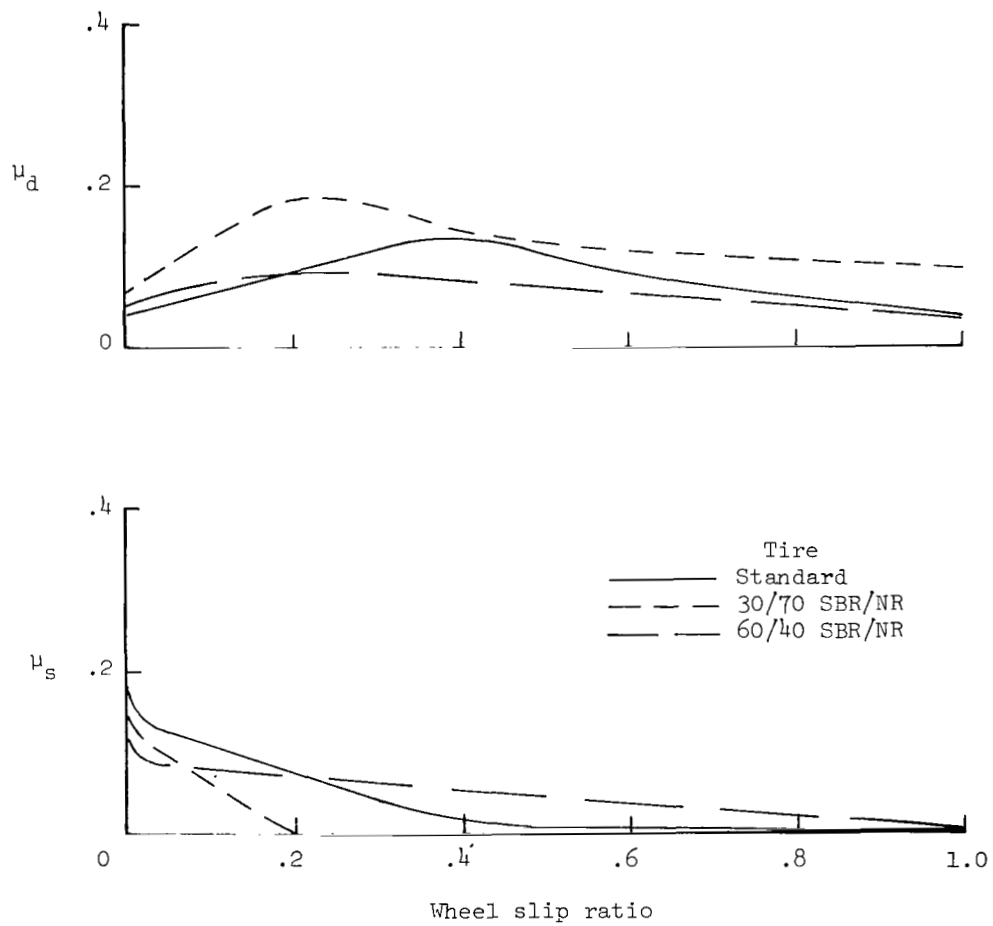


Figure 7.- Variation of computed friction coefficients with wheel slip ratio during brake cycle on dry concrete. Yaw angle, 10.9° ; ground speed, 106 knots.



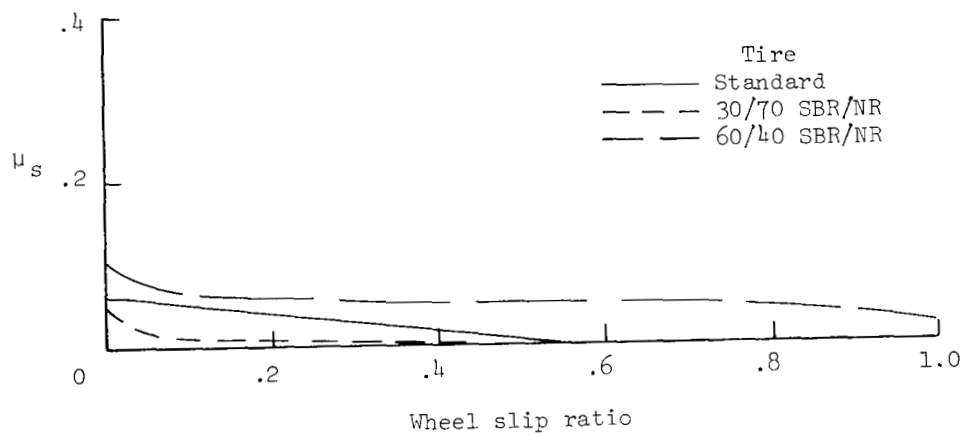
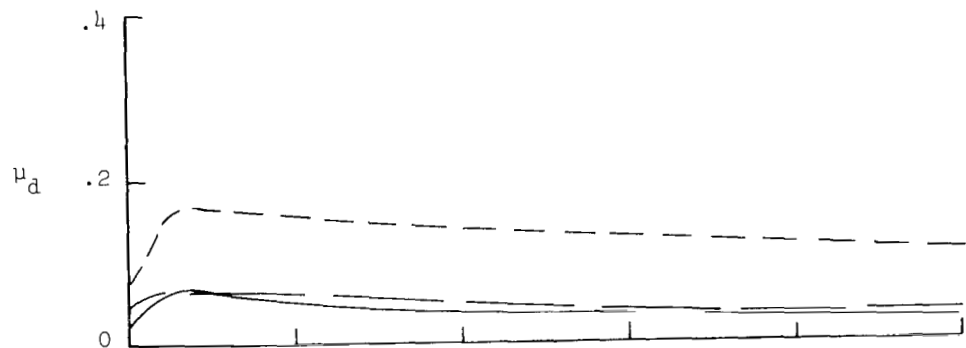
(a) Dry concrete surface.

Figure 8.- Variation of drag-force friction coefficient μ_d and cornering-force friction coefficient μ_s with wheel slip ratio for three test tires on dry, damp, and flooded concrete surfaces. Ground speed, ≈ 100 knots; yaw angle, 10.9° .



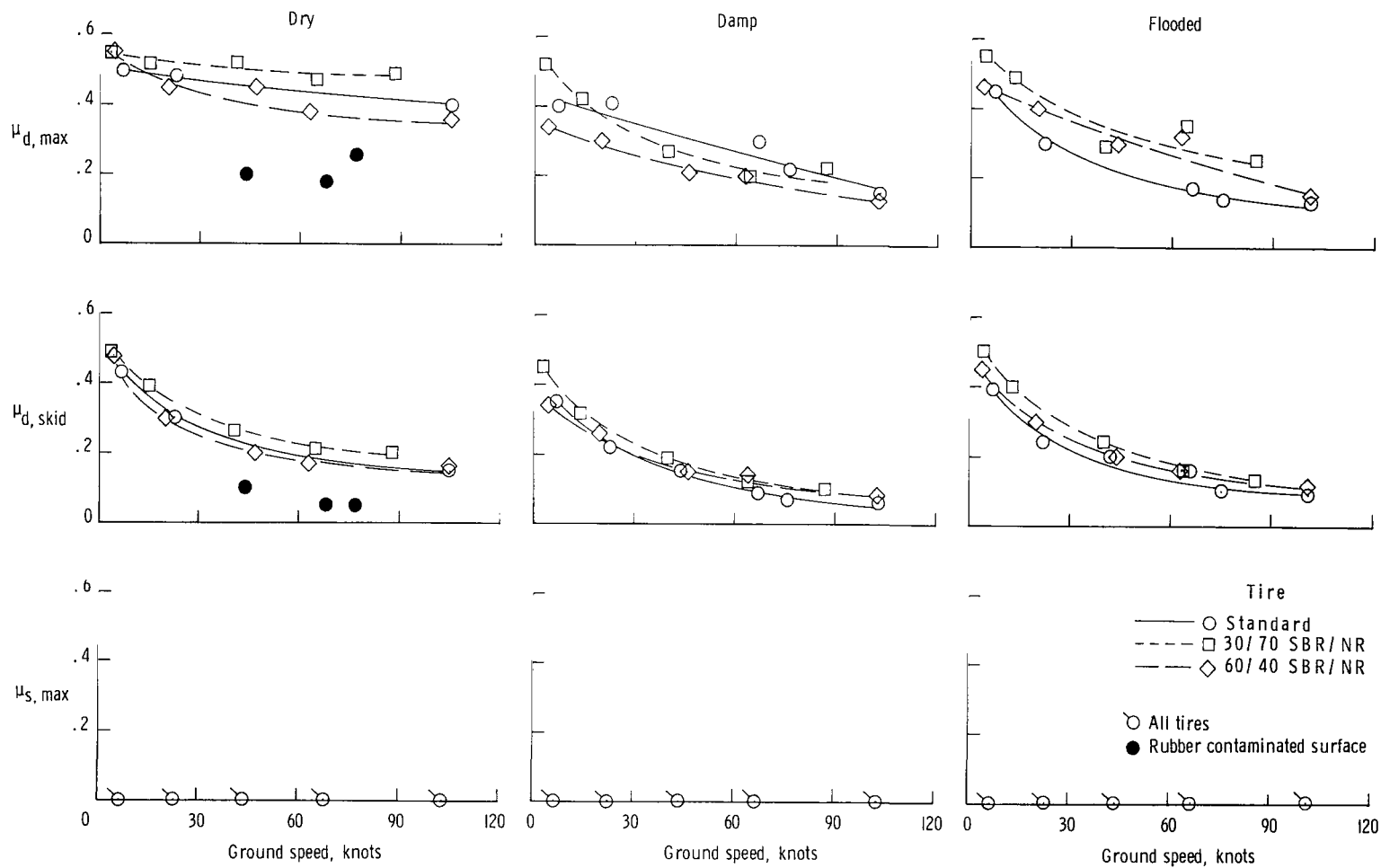
(b) Damp concrete surface.

Figure 8.- Continued.



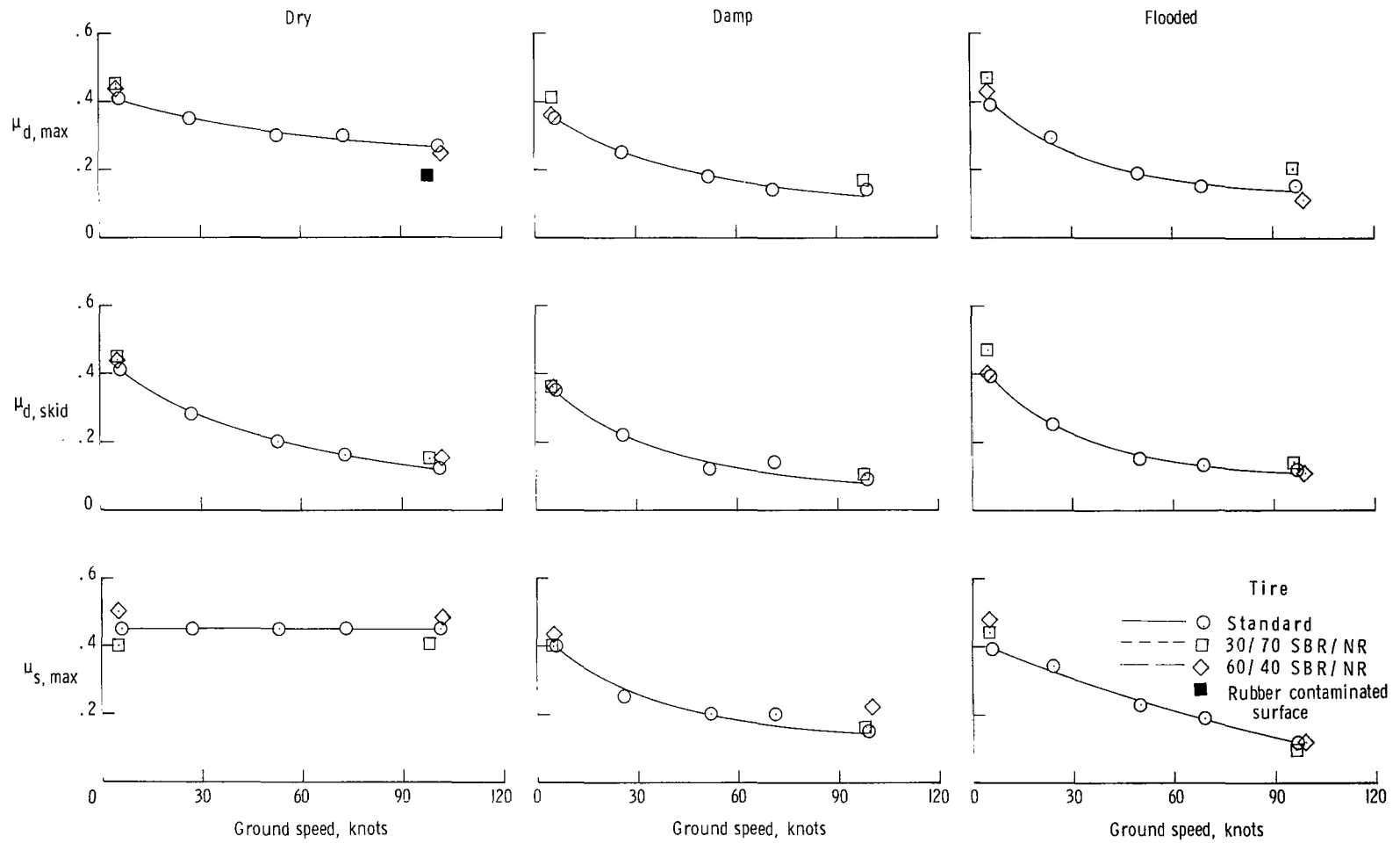
(c) Flooded concrete surface.

Figure 8.- Concluded.



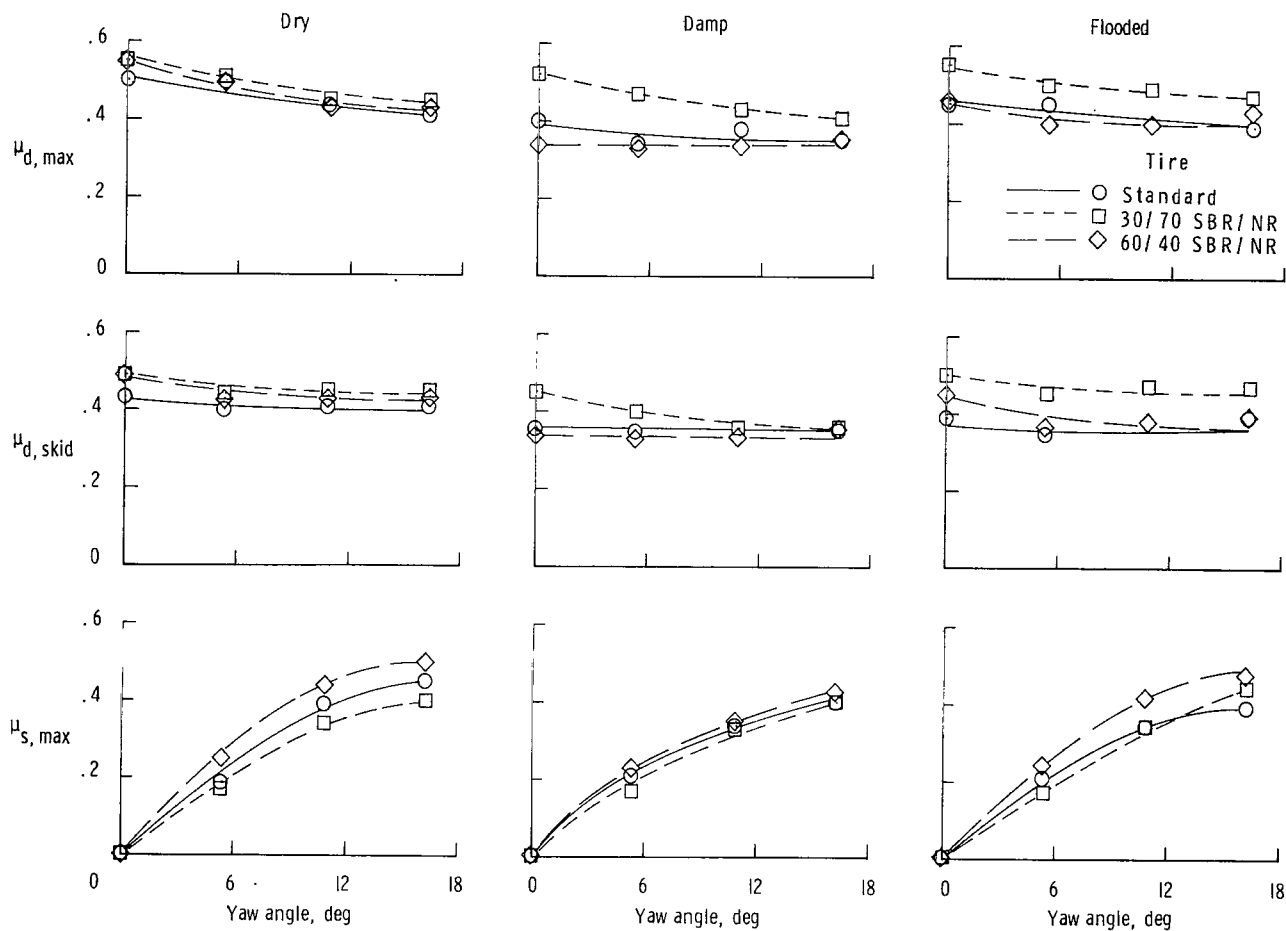
(a) Yaw angle = 0° .

Figure 9.- Effect of ground speed on maximum drag-force friction coefficient $\mu_{d,max}$, skidding drag-force friction coefficient $\mu_{d,skid}$, and maximum cornering-force friction coefficient $\mu_{s,max}$ at two yaw angles for three test tires on dry, damp, and flooded surfaces.



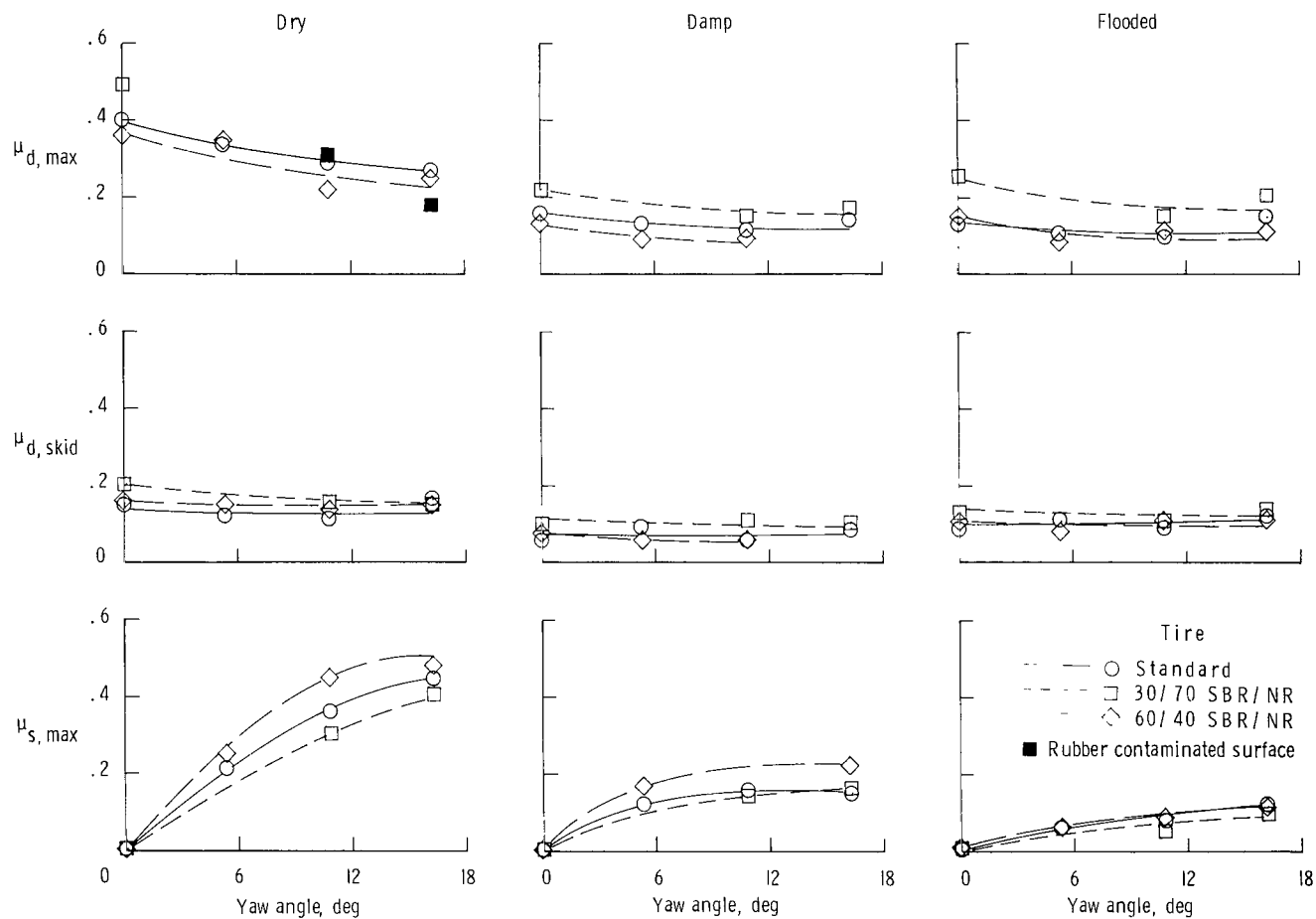
(b) Yaw angle = 16.3°.

Figure 9.- Concluded.



(a) Ground speed \approx 5 knots.

Figure 10.- Effect of yaw angle on maximum drag-force friction coefficient $\mu_{d,max}$, skidding drag-force friction coefficient $\mu_{d,skid}$, and maximum cornering-force friction coefficient $\mu_{s,max}$ at two ground speeds for three test tires on dry, damp, and flooded surfaces.



(b) Ground speed \approx 100 knots.

Figure 10.- Concluded.



584 001 C1 U A 760611 S00903DS
DEPT OF THE AIR FORCE
AF WEAPONS LABORATORY
ATTN: TECHNICAL LIBRARY (SUL)
KIRTLAND AFB NM 87117

POSTMASTER: If undeliverable (Section 158
Postal Manual) Do Not Return

"The aeronautical and space activities of the United States shall be conducted so as to contribute . . . to the expansion of human knowledge of phenomena in the atmosphere and space. The Administration shall provide for the widest practicable and appropriate dissemination of information concerning its activities and the results thereof."

—NATIONAL AERONAUTICS AND SPACE ACT OF 1958

NASA SCIENTIFIC AND TECHNICAL PUBLICATIONS

TECHNICAL REPORTS: Scientific and technical information considered important, complete, and a lasting contribution to existing knowledge.

TECHNICAL NOTES: Information less broad in scope but nevertheless of importance as a contribution to existing knowledge.

TECHNICAL MEMORANDUMS: Information receiving limited distribution because of preliminary data, security classification, or other reasons. Also includes conference proceedings with either limited or unlimited distribution.

CONTRACTOR REPORTS: Scientific and technical information generated under a NASA contract or grant and considered an important contribution to existing knowledge.

TECHNICAL TRANSLATIONS: Information published in a foreign language considered to merit NASA distribution in English.

SPECIAL PUBLICATIONS: Information derived from or of value to NASA activities. Publications include final reports of major projects, monographs, data compilations, handbooks, sourcebooks, and special bibliographies.

TECHNOLOGY UTILIZATION PUBLICATIONS: Information on technology used by NASA that may be of particular interest in commercial and other non-aerospace applications. Publications include Tech Briefs, Technology Utilization Reports and Technology Surveys.

Details on the availability of these publications may be obtained from:

SCIENTIFIC AND TECHNICAL INFORMATION OFFICE

NATIONAL AERONAUTICS AND SPACE ADMINISTRATION

Washington, D.C. 20546